NOTE: This is the accepted version of the paper, to appear in IEEE Transactions on Magnetics. The published version will be available at:
http://dx.doi.org/10.1109/TMAG.2013.2260348

Improvised Open Boundary Conditions for Magnetic Finite Elements

David Meeker, *Member, IEEE*

***Abstract*—Although sparse, exact open boundary methods exist, the implementation of these methods requires capabilities that are not present in all finite element solvers. This work describes methods for the implementation of accurate higher-order asymptotic boundary conditions for 2D planar, axisymmetric, and 3D magnetostatic problems that can be improvised in virtually any finite element program.**

I. Introduction

In many cases, it is desirable to solve magnetostatic or quasi-static problems on an unbounded domain. If finite element methods are used, however, the domain must be truncated to a bounded region in order to yield a solvable problem. The need to approximate the solution of an unbounded domain via finite elements has led to a variety of "open boundary" methods [1].

Sparse, exact open boundary methods exist (*i.e.* the Kelvin transformation [2] [3] and related mapping methods [4]), and these methods are widely implemented in commercial solvers. However these methods rely on features that may not be present in simpler codes, namely periodic boundary conditions and material properties that vary as a smooth function of position.

The Charge Iteration approach [5] is also sparse and exact and does not require periodic boundary conditions or position-dependent material properties. However, several iterations are typically required for the boundary charge distribution to converge, and additional code is required to update the boundary charges between iteration.

Asymptotic boundary conditions (ABCs) are a sparse but approximate open boundary method [6] [7]. The magnetic field could be viewed as a set of harmonics, the magnitude of each harmonic decaying to zero with increasing distance from the objects of interest. ABCs rely on the fact that at a modest distance, higher-order harmonics have mostly decayed, and the field is dominated by a small number of lower-order harmonics. ABCs accurately emulate the impedance of unbounded space for the low-order harmonics at the finite element domain's artificial outer boundary. It is assumed that the negligible error is introduced by not exactly modeling the boundary impedance for higher-order harmonics. First-order ABCs specify the parameters of a mixed-type boundary condition that matches the far-field characteristics of a magnetic dipole. While higher-order ABCs that emulate the far-field behavior of multipoles are possible and provide improved accuracy, these boundary conditions have been less commonly seen because low-level code modifications were presented in previous works as their method of implementation.

This work presents an "improvised" realization of first-, second-, and third-order ABCs in 2D, axisymmetric, and 3D finite element problems. These boundary conditions can be realized using only basic functionality that exists in virtually any finite element solver, and no extra iteration is required. The finite element domains under consideration have a circular or spherical outer boundary. The open boundary is emulated by placing thin layers of isotropic material at the outer extents of the domain. By careful selection of the magnetic permeability of the layers, ABCs are produced. This method allows for accurate open-boundary solutions with nearby boundaries. The proposed method is distinct from static "Perfectly Matched Layer" approaches described in [8]–[10] because the layers employed in the proposed approach are isotropic rather than anisotropic; fine meshing is not a prerequisite in the boundary layers; and the proposed method is derived from ABCs. The performance of the proposed method is demonstrated by example problems.

II. First-Order 2D Boundary Condition

The simplest improvised boundary condition results from a first-order ABCs for a 2D planar magnetic problem. In polar coordinates, the general solution for magnetic vector potential, A, in which $A \to 0$ at infinity is [6]:

$$A(\rho, \phi) = \sum_{n=1}^{\infty} \frac{a_n(\phi)}{\rho^n} \tag{1}$$

where ρ and ϕ are the radius and angle that define the polar coordinate system. By differentiating (1) with respect to ρ, it can be concluded that:

$$\frac{\partial A_n}{\partial \rho} = -\frac{nA_n}{\rho} \tag{2}$$

where A_n represents the vector potential contribution of the n^{th} harmonic.

If a circular boundary is employed, eq. (2) with $n = 1$ is a directly applicable open boundary condition. If a particular code does not support Robin-type boundary conditions, (2) can be implemented by defining, as shown in Figure 1, an annular region of thickness d and magnetic permeability μ_1 outside the circular region of interest. The Dirichlet boundary condition $A = 0$ is defined on the exterior of the annulus. In the Figure, x and y refer to the axes in the 2D planar case. The same figure can be drawn for the axisymmetric case, re-labeling the axes as r and z.

The permeability of the annulus can be obtained by considering the analytical solution to the field in the annulus.

D. Meeker is with QinetiQ North America, 350 Second Ave, Waltham, MA, 02451 USA e-mail: dmeeker@ieee.org.

Manuscript received February 14, 2013

From [11], the general solution for a 2D Laplace equation in polar coordinates on a bounded circle is:

$$A_n = a_n(\phi)\left(c_1(n)\rho^n + c_2(n)\rho^{-n}\right) \tag{3}$$

for $n = 1 \ldots \infty$, where $a_n(\phi)$ is strictly a function of angle and $c_1(n)$ and $c_2(n)$ are constants for the n^{th} harmonic that are determined on the basis of the boundary conditions:

$$A_1(R) = a_1(\phi)/R \tag{4}$$

$$A_1(R+d) = 0 \tag{5}$$

Solving for c_1 and c_2 and substituting into (3) yields:

$$A_1 = \frac{a_1(\phi)}{R}\left(\frac{R(d-\rho+R)(d+\rho+R)}{\rho d(d+2R)}\right) \tag{6}$$

By differentiating (6) with respect to ρ, it can be concluded that at the $\rho = R_+$:

$$\left.\frac{\partial A_1}{\partial \rho}\right|_{\rho=R_+} = -\left(\frac{\delta^2+2\delta+2}{\delta(\delta+2)}\right)\frac{A_1}{R} \tag{7}$$

where $\delta = d/R$.

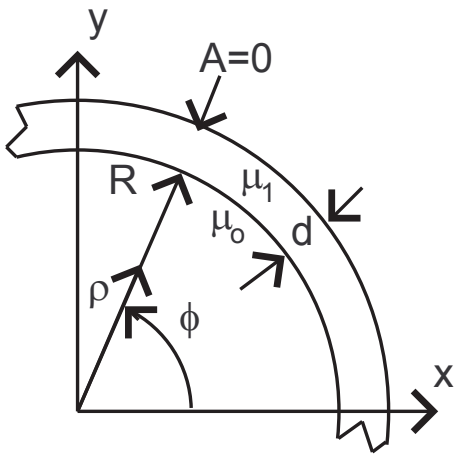

Fig. 1. First order 2D planar improvised boundary condition.

Eq. (7) has the same form as the desired boundary condition (2), but (7) applies at the $\rho = R+$ side of the boundary between the domain and the annulus. To link the domain of interest to the annular region at $\rho = R$, continuity of tangential field intensity, H_t, is invoked from [12]:

$$H_t = -\frac{1}{\mu_o}\left.\frac{\partial A_1}{\partial \rho}\right|_{\rho=R_-} = -\frac{1}{\mu_1}\left.\frac{\partial A_1}{\partial \rho}\right|_{\rho=R_+} \tag{8}$$

Eq. (8) can then be combined with (7) to write the boundary condition in terms of quantities at the $\rho = R_-$ side of the interface:

$$\left.\frac{1}{\mu_o}\frac{\partial A_1}{\partial \rho}\right|_{\rho=R_-} = -\frac{1}{\mu_1}\left(\frac{\delta^2+2\delta+2}{\delta(\delta+2)}\right)\frac{A_1}{R} \tag{9}$$

The desired ABC, eq. (2), is equal (9) if the permeability of the annular region is selected to be:

$$\frac{\mu_1}{\mu_o} = \frac{\delta^2+2\delta+2}{\delta(\delta+2)} \tag{10}$$

If δ is small, (10) is well-approximated by the first term in its series expansion:

$$\frac{\mu_1}{\mu_o} \approx \frac{1}{\delta} \tag{11}$$

III. First-Order Axi/3D Boundary Condition

Calculation of a first-order boundary condition for the axisymmetric case is very similar. The general solution for the far-field, analogous to (1), is:

$$A(\rho,\phi) = \sum_{n=1}^{\infty}\frac{a_n(\phi)}{\rho^{n+1}} \tag{12}$$

for the axisymmetric case, where ρ is the the radial distance and ϕ is the polar angle in a spherical coordinate system and vector potential A has only one the azimuthally-directed component. By differentiating (12) with respect to ρ, it can be concluded that the applicable boundary condition is:

$$\frac{\partial A_n}{\partial \rho} + \frac{A_n}{\rho} = -\frac{nA_n}{\rho} \tag{13}$$

The general solution in the annulus has the form [12]:

$$A_n = a_n(\phi)\left(c_1(n)\rho^n + c_2(n)\rho^{-(n+1)}\right) \tag{14}$$

In the axisymmetric case, the tangential portion of the field intensity at the boundary is [12]:

$$H_t = -\frac{1}{\mu_o}\left.\left(\frac{\partial A}{\partial \rho} + \frac{A}{\rho}\right)\right|_{\rho=R_-} \tag{15}$$

Solving for c_1 and c_2 as before and applying continuity of H_t leads to:

$$\frac{\mu_1}{\mu_o} = \frac{\delta^3+3\delta^2+3\delta+3}{\delta\left(\delta^2+3\delta+3\right)} \tag{16}$$

The small δ approximation of (16) is identical to (11).

Since the spherical boundary region has no particular orientation dependence, the solution for the axisymmetric case can also be used for 3D models.

IV. Higher Order 2D Boundary Conditions

The first-order ABC realization is easily implemented and useful in itself. However, accuracy breaks down if the objects in the domain of interest are not dipole-like: if the objects aren't centered in the domain or if significant higher harmonics are present. To ease these restrictions, higher-order ABCs are needed. The second-order case will be considered here in detail, but the same method can be used for higher-order boundary conditions by adding additional layers to the boundary condition. For example, instead of picking the boundary to match the behavior of a dipole, the second-order ABC matches the behavior of both a dipole and a quadrupole. The first-order ABC was realized using a circular boundary surrounded by a thin annular region of higher permeability. To satisfy a second-order ABC, it is assumed that the boundary condition can be created using a two-layer region, as shown in Figure 2. Each of the layers has thickness d. The inner layer has permeability

μ_1 and the outer layer has permeability μ_2. The task is select the permeability of the two layers so that the second-order ABC is realized.

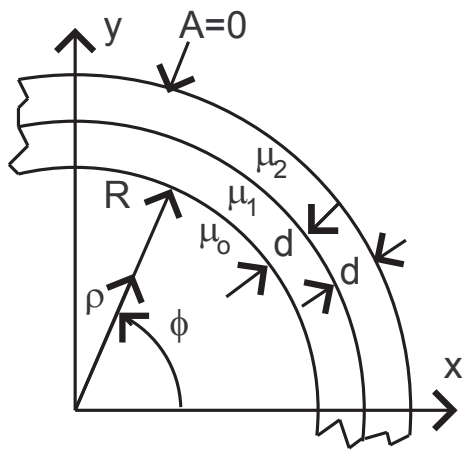

Fig. 2. Second order 2D planar improvised boundary condition.

Following the general solution from (3), separate solutions, A_i and A_o are written for the inner and outer layers respectively:

$$A_i = a_n(\phi)\left(c_{11}(n)\rho^n + c_{21}(n)\rho^{-n}\right) \quad (17)$$

$$A_o = a_n(\phi)\left(c_{12}(n)\rho^n + c_{22}(n)\rho^{-n}\right) \quad (18)$$

A set of four equations can then be formed by applying continuity of normal flux density and tangential field intensity at the interface between the two layers:

$$A_i(R) = a_n(\phi)/R \quad (19)$$

$$A_i(R+d) = A_o(R+d) \quad (20)$$

$$\frac{1}{\mu_1}\frac{\partial A_i}{\partial \rho}(R+d) = \frac{1}{\mu_2}\frac{\partial A_o}{\partial \rho}(R+d) \quad (21)$$

$$A_o(R+2d) = 0 \quad (22)$$

Using a symbolic manipulator, an analytical solution for $c_{11}(n)$, $c_{21}(n)$, $c_{21}(n)$, and $c_{22}(n)$ was obtained.

Two more equations can then be written to determine the permeability of each layer by applying (2) for $n = 1, 2$:

$$-H_t|_{n=1} = \frac{1}{\mu_1}\left.\frac{\partial A_i}{\partial \rho}(R)\right|_{n=1} = -A_1(R)/(\mu_o R) \quad (23)$$

$$-H_t|_{n=2} = \frac{1}{\mu_1}\left.\frac{\partial A_i}{\partial \rho}(R)\right|_{n=2} = -2A_2(R)/(\mu_o R) \quad (24)$$

Eqs. (23) and (24) can again be solved with the aid of a symbolic manipulator. However, the analytical solution is not compact nor convenient. Table I lists evaluations of the analytical solution for a wide range of δ. Taking the limit as boundary thickness $\delta \to 0$ does yield a convenient form, however. The small δ limit is presented as the first row of the table. Higher order ABCs can be generated by applying additional continuity conditions (20) and (21) at the interfaces between the additional boundary layers. Table I also presents the analogous results for a third-order ABC.

TABLE I
2ND AND 3RD ORDER 2D SOLUTIONS.

	2rd Order		3rd Order		
δ	μ_1/μ_o	μ_2/μ_o	μ_1/μ_o	μ_2/μ_o	μ_3/μ_o
$\delta \to 0$	$3\,\delta$	$3/(2\,\delta)$	$1/(6\delta)$	$(10\,\delta)/6$	$10/(6\delta)$
0.001	0.00299849	1502.25	166.752	0.00166418	1670.83
0.0025	0.0074905	602.245	66.755	0.00415127	670.829
0.005	0.0149615	302.239	33.4266	0.00827262	337.491
0.01	0.0298421	152.229	16.7699	0.0164308	170.815
0.025	0.0739412	62.1965	6.79961	0.0403162	70.7882
1/30	0.0980491	47.1786	5.1494	0.053269	54.1064
0.05	0.145314	32.1429	3.51534	0.0786636	37.4093
0.1	0.278128	17.0384	1.94234	0.152429	20.6497
0.25	0.580487	7.78137	1.16242	0.358465	10.3724
0.5	0.825804	4.56166	1.02427	0.598073	6.70408
1	0.957203	2.96581	1.002	0.79096	4.76838

TABLE II
2ND AND 3RD ORDER AXISYMMETRIC SOLUTIONS.

	2rd Order		3rd Order		
δ	μ_1/μ_o	μ_2/μ_o	μ_1/μ_o	μ_2/μ_o	μ_3/μ_o
$\delta \to 0$	$4\,\delta$	$2/\delta$	$1/(7\delta)$	$(120\,\delta)/49$	$20/(7\delta)$
0.001	0.00399599	2000	142.86	0.00244168	2857.15
0.0025	0.00997481	800	57.1495	0.00607731	1142.87
0.005	0.0198985	400	28.5848	0.0120674	571.45
0.01	0.0395883	200	14.3124	0.0238035	285.757
0.025	0.0973252	79.9991	5.78115	0.0573497	114.392
1/30	0.128485	59.9986	4.37479	0.075118	85.8557
0.05	0.188706	39.9975	2.99018	0.109309	57.3539
0.1	0.351313	19.9973	1.68571	0.205825	28.9765
0.25	0.679867	8.05042	1.09427	0.459607	12.2409
0.5	0.894833	4.24456	1.01053	0.709899	6.91301
1	0.981767	2.58334	1.00058	0.872702	4.49224

V. HIGHER ORDER AXI/3D BOUNDARY CONDITIONS

The solution for the second-order axisymmetric case proceeds very much like the 2D case, substituting the solution (14) for (3) and substituting the axisymmetric definition of tangential field intensity (15) for the 2D version in (23) and (24). Again, a symbolic manipulator is required to solve the six equations for c_{11} - c_{22}, μ_1, and μ_2, and the closed-form solutions for permeability of the external regions are not convenient. Second and third-order results are presented for a wide range of δ in Table II.

VI. OPEN BOUNDARY EXAMPLES

A. Axisymmetric Example

An illustrative example is presented in [3]. A 1000-turn coil with a 4m outer diameter, a 2m inner diameter, and a 1m axial length is enclosed in a spherical domain 5m in diameter. The objective is to find the inductance of the coil, exercising various open boundary strategies. In this example, the outer boundary is very close to and strongly affects the inductance of the coil.

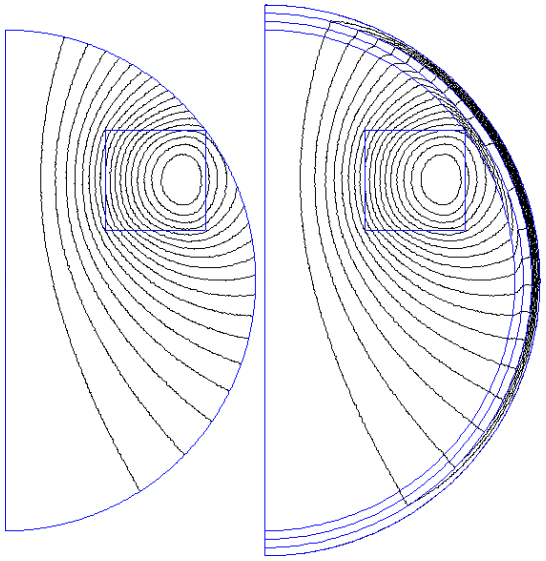

Fig. 3. Kelvin Transformation and 3rd order ABC solutions.

In [3], the inductance of the coil is only considered at the center of the spherical domain. Here, to provide a better comparison between various boundary condition orders, the inductance is considered over a range of coil positions. The coil position varies from $0\,m$ (centered in the domain) to $1\,m$ (in contact with the outer boundary). An accurate open boundary method should produce very nearly the same inductance result regardless of the position in the domain. In the present example, δ was selected so that the total boundary stack-up is 1/10 of the radius of the problem domain.

FEMM [13] was used to simulate 1st through 3rd order ABCs and Kelvin Transformation BCs for various coil offsets. The domains were meshed finely enough so that boundary conditions are the dominant source of error in the example problems. First order triangular mesh with about 40,000 node points per solution were employed (with about 80,000 nodes required for a comparable Kelvin Transformation solution, since the exterior domain was meshed at the same mesh size as the interior).

Representative simulation results are shown in Figure 3, which compares the flux lines computed by applying exact Kelvin Transformation method to those from an improvised 3rd order ABC. In Figure 3, there is no visual difference in the solutions, even though the coil is in contact with the boundary.

The simulation results for all simulations are summarized in Figure 4. In the figure, inductance results are normalized by the average of the results from simulations with a Kelvin-type open boundary boundary condition over the range of possible coil displacements.

Since the Kelvin Transformation is an exact representation of all space, Figure 4 confirms that solution has essentially no dependence on position. A small level of error is still present, however, due to mesh discretization. The "improvised" boundary conditions show better performance as the order of the boundary condition is increased. The 3rd order boundary performs well across a wide range of displacements; inductance error with the coil touching the boundary is only 0.1%.

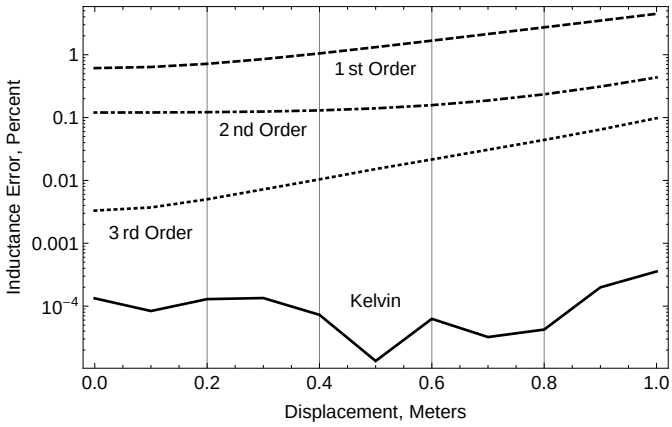

Fig. 4. Inductance error vs. position for example problem.

TABLE III
LOSSES COMPUTED WITH VARIOUS BOUNDARY CONDITIONS.

BC Type	Mesh Nodes	Loss (W/m)	Energy (J/m)
Kelvin	22342	66.508	0.263366
3rd Order ABC	13642	66.502	0.264313
2nd Order ABC	13007	66.527	0.259605
1st Order ABC	12790	67.074	0.275513
Dirichlet	11489	67.754	0.167933
Neumann	11489	71.941	0.351713

B. 2D Example

A 2D time-harmonic simulation of three-phase busbars is motivated by [14]. Three solid copper busbars with a 50mm width and 6mm thickness are located in unbounded space with a 70mm separation between bars. The busbars have a conductivity of 58MS/m and carry 60 Hz net currents of $848\,A_{pk} * \{e^{-2j\pi/3}, 1, e^{2j\pi/3}\}$.

The busbars are subject to skin and proximity effect eddy currents which result in increased losses. To accurately predict both the losses and the stored energy, an open boundary simulation is required. Various boundary conditions were applied to the problem with a Kelvin Transformation solution used as a benchmark. For the improvised ABC solutions, δ was selected so that the total boundary stack-up is 1/10 of the radius of the problem domain.

Plots of the real and imaginary portions of the flux lines are shown in Figure 5 and 6 respectively. As demonstrated by the plots, the real portion of the flux lines are dominated by the 2^{nd} harmonic, whereas the imaginary portions of the flux lines are dominated by the 1^{st} harmonic.

Average loss and stored energy for various boundary condition assumptions are listed in Table III. The 2^{nd} and 3^{rd} order ABC losses closely match those predicted by the Kelvin BC case, because these ABCs can reproduce the leading 1X and 2X harmonics exhibited by the problem. The 1st order ABC is less accurate because it cannot accurately reproduce the 2X field associated with the real part of the solution. However, the 1st order ABC still has improved accuracy versus both the Dirichlet and Neumann conditions.

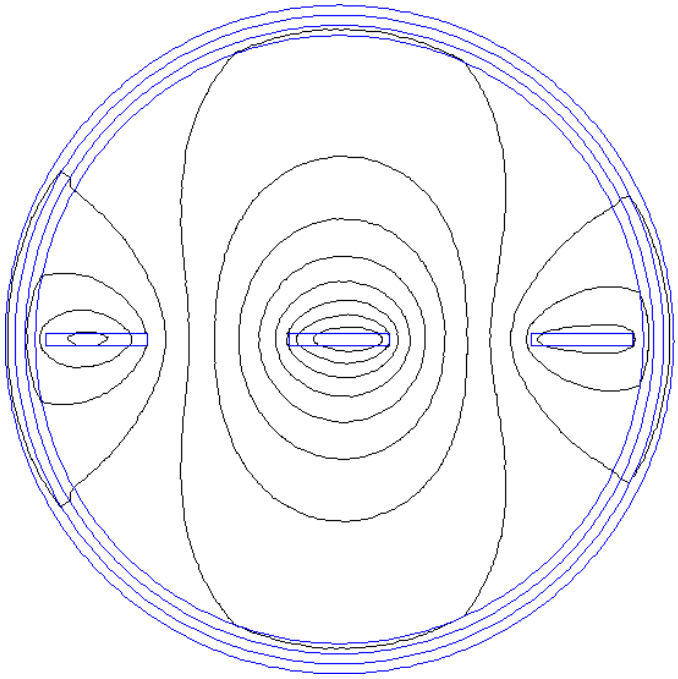

Fig. 5. Real flux lines for AC busbar example.

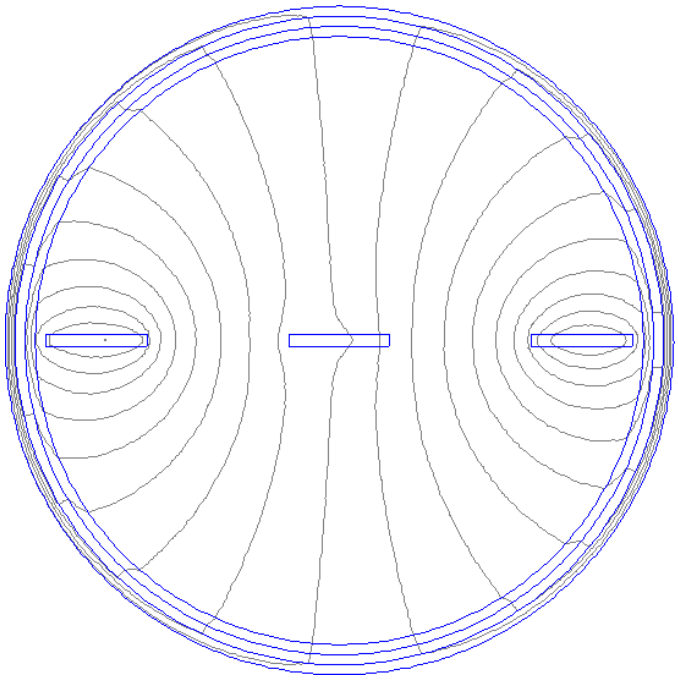

Fig. 6. Imaginary flux lines for AC busbar example.

VII. Conclusions

Improvised versions of asymptotic boundary conditions for 2D, axisymmetric, and 3D low frequency magnetic problems have been presented. The proposed method enables accurate solutions to unbounded problems, and the method can be employed in an ad-hoc fashion in virtually any finite element solver.

For many practical cases, the boundary is not drawn so close as in the present examples. Then, the two-layer, second-order boundary may be a good compromise between ease of implementation, domain size, and accuracy. Higher order ABCs can be used where accuracy approaching that of the Kelvin Transformation is desired.

Although the example problems presented in this work contain no magnetically permeable or nonlinear materials, nothing in the proposed method restricts their use. The proposed improvised ABCs require no additional operations nor iterations that might adversely affect the convergence of solutions with nonlinear materials.

For problems with symmetry, Neumann and/or Dirichlet conditions can be used in combination with improvised ABCs to truncate the problem domain *e.g.* into a half or quarter circle. Depending upon the specific problem, particular harmonics may be forced to zero through the choice of the Neumann and/or Dirichlet boundary conditions. In those cases, improved accuracy can be obtained by deriving improvised ABCs that match a different set of harmonics than the ones considered in the present work. For example, one might desire a second order ABC to match the 1^{st} and 3^{rd} harmonics rather than the 1^{st} and 2^{nd} in a case where odd symmetry is enforced by the choice of boundary conditions.

The approach in this paper applied a $B \cdot n = 0$ boundary condition on the outer edge of the boundary region. Another possible derivation would apply $H \times n = 0$ instead. This alternate derivation might have advantages with alternative finite element formulations, *e.g.* edge element formulations or scalar potential formulations.

Extensions to the current work could present even higher-order results; apply the formulation to other related areas like electrostatics/quasistatics or heat conduction; or explore approaches to "improvised" implementation of a ABCs to non-circular boundaries.

References

[1] Q. Chen and A. Konrad, "A review of finite element open boundary techniques for static and quasi-static electromagnetic field problems," *IEEE Trans. Magn.*, vol. 33, pp. 663–676, Jan. 1997.

[2] E. M. Freeman and D. A. Lowther, "A novel mapping technique for open boundary finite element solutions to Poissons equation," *IEEE Trans. Magn.*, vol. 24, pp. 2934–2936, Nov. 1988.

[3] E.M. Freeman, and D. A. Lowther, "An open boundary technique for axisymmetric and three dimensional magnetic and electric field problems," *IEEE Trans. Magn.*, vol. 25, pp. 4135–4137, Sept. 1989.

[4] Imhoff, J. F. *et al.*, "An original solution for unbounded electromagnetic 2d and 3d problems throughout the finite element method," *IEEE Trans. Magn.*, vol. 26, pp. 1659–1661, Sept. 1990.

[5] G. Aiello *et al.*, "Finite element analysis of unbounded non-linear transient magnetic fields," *IEEE Trans. Magn.*, vol. 33, pp. 1318–1321, Mar. 1997.

[6] Q. Chen, A. Konrad, and P. P. Biringer, "Computation of static and quasistatic electromagnetic fields using asymptotic boundary conditions," *Applied Computational Electromagnetics Society Journal*, vol. 9, pp. 37–42, July 1994.

[7] S. Gratkowski, L. Pichon, and H. Gajan, "Asymptotic boundary conditions for open boundaries of axisymmetric magnetostatic finite-element models," *IEEE Trans. Magn.*, vol. 38, pp. 469–472, Mar. 2002.

[8] I. Bardi, O. Biro, and K. Preis, "Perfectly matched layers in static fields," *IEEE Trans. Magn.*, vol. 34, pp. 2433–2436, Sept. 1998.

[9] L. Dedek, J. Dedkova, and J Valsa, "Optimization of perfectly matched layer for Laplace's equation," *IEEE Trans. Magn.*, vol. 38, pp. 501–504, Mar. 2002.

[10] S. Alfonzetti, and G. Borzi, "Perfectly matched layer for static and quasistatic fields: a false method," *IEEE Trans. Magn.*, vol. 39, pp. 1115–1118, May 2003.

[11] R. Haberman, *Elementary Applied Partial Differential Equations*, 2nd ed., Prentice-Hall, 1987.
[12] J. D. Jackson, *Classical Electrodynamics*, 3rd ed., Wiley, 1999.
[13] D. C. Meeker, *Finite Element Method Magnetics*, Version 4.2 (11Apr2012 Build), http://www.femm.info
[14] M. Imamura *et al.*, "Analysis of magnetic fields due to three-phase bus bar currents for the design of an optical current transformer," *IEEE Trans. Magn.*, vol. 34, pp. 2274–2279, July 1998.